https://doi.org/10.5194/bg-2021-312
Preprint. Discussion started: 3 January 2022

Biogeosciences Discussions
Open Access
EGU

Investigating the effect of nickel concentration on phytoplankton growth to inform the assessment of ocean alkalinity enhancement

Jiaying Abby Guo[1], Robert Strzepek[2], Anusuya Willis[3], Aaron Ferderer[1], Lennart Thomas Bach[1]

1 Institute for Marine and Antarctic Studies, University of Tasmania, Hobart, Tasmania, Australia

2 Australian Antarctic Program Partnership (AAPP), Institute for Marine and Antarctic Studies, University of Tasmania, Hobart, Tasmania, Australia

3 National Collections and Marine Infrastructure, Commonwealth Scientific and Industrial Research Organisation, Hobart, Tasmania, Australia

Correspondence to: Jiaying Abby Guo (jiaying.guo@utas.edu.au)

Abstract. Ocean alkalinity enhancement (OAE) is a proposed method for removing carbon dioxide (CO_2) from the atmosphere by the accelerated weathering of (ultra-) basic minerals to increase alkalinity – the chemical capacity of seawater to store CO_2. During the weathering of OAE-relevant minerals relatively large amounts of trace metals will be released and may perturb pelagic ecosystems. Nickel (Ni) is of particular concern as it is abundant in olivine, one of the most widely considered minerals for OAE. However, so far there is limited knowledge about the impact of Ni on marine biota including phytoplankton. To fill this knowledge gap, this study tested the growth and photo-physiological response of 11 marine phytoplankton species to a wide range of dissolved Ni concentrations (from 0.07 nmol/L to 50,000 nmol/L). We found that the phytoplankton species were not very sensitive to Ni concentrations under the culturing conditions established in our experiments, but the responses were species-specific. The growth rates of 6 of the 11 tested species showed small but significant responses to changing Ni concentrations. Photosynthetic performance, assessed by measuring the maximum quantum yield (F_v/F_m) and the functional absorption cross-section (σ_{PSII}) of photosystem II, was also only mildly sensitive to changing Ni in 3 out of 11 species and 4 out of 11 species, respectively. The limited effect of Ni may be partly due to the provision of nitrate as the nitrogen source for growth, as previous studies suggest higher sensitivities when urea is the nitrogen source. Furthermore, limited influence may be due to the relatively high concentrations of organic ligands in the growth media in our experiments. These ligands reduced bioavailable Ni (i.e., "free Ni^{2+}") concentrations by binding the majority of the dissolved Ni. Our data suggest that dissolved Ni

https://doi.org/10.5194/bg-2021-312
Preprint. Discussion started: 3 January 2022

does not have a strong effect on phytoplankton under our experimental conditions, but we emphasize that a deeper understanding of nitrogen sources, ligand concentrations and phytoplankton composition is needed when assessing the influence of Ni release associated with OAE. We discuss if applications of OAE with Ni-rich minerals may be safer in regions with high organic ligand concentrations and low concentrations of urea as such boundary conditions may lead to less impact of Ni on phytoplankton communities.

1 Introduction

Increased burning of fossil fuels and land-use changes have resulted in a significant increase in atmospheric CO_2 from a preindustrial value of ~280 ppm to currently ~415 ppm (Friedlingstein et al., 2020). Detrimental effects of rising CO_2 include global warming, increasing sea levels, ocean acidification and more frequent extreme weather (IPCC, 2019). To limit detrimental impacts, CO_2 emissions must be rapidly reduced. Additionally, about 100-1000 gigatonnes (Gt) of CO_2 must be removed from the atmosphere by 2100 and permanently stored in other reservoirs (Rogelj et al., 2016). One potential method for the required atmospheric CO_2 removal (CDR) is to increase ocean alkalinity thereby increasing the chemical capacity of seawater to permanently store CO_2 (Kheshgi, 1995). Alkalinity is formed naturally during the chemical weathering of certain minerals such as olivine (Schuiling and Krijgsman, 2006). Chemical rock weathering will absorb most of the anthropogenic CO_2, but only over a period of tens- to hundreds-thousand years (Archer et al., 2009). “Ocean alkalinity enhancement (OAE)” and “enhanced weathering (EW)” seek to accelerate natural rock weathering processes by spreading pulverized minerals onto the ocean surface (in the case of OAE) or warm and humid land areas (in the case of EW) (Schuiling and Krijgsman, 2006; Kheshgi, 1995). Modelling studies suggest that OAE and EW can help to mitigate climate change significantly when operated at an appropriate scale (Lenton et al., 2018; Ilyina et al., 2013; Kohler et al., 2010).

A variety of trace metals are released into the environment alongside alkalinity during chemical weathering. The quality and quantity of released trace metals depends on the mineral used for OAE or EW. Olivine is currently one of the most widely considered minerals due to its relatively fast weathering rates (Taylor et al., 2016). It contains high amounts of nickel (Ni), which was shown to leach out of olivine faster than alkalinity during chemical weathering (Montserrat et al., 2017). Thus, the potentially large amounts of Ni released into the environment are a predominant environmental concern of EW or OAE with olivine (Hartmann et al., 2013; Bach et al., 2019). In the case of EW, Ni would first affect terrestrial ecosystems but a fraction of it would be transported into the oceans via rivers. In the case of OAE, Ni would directly affect marine biota. Phytoplankton are at the base of the marine

https://doi.org/10.5194/bg-2021-312
Preprint. Discussion started: 3 January 2022

food web so that it is central to the assessment of EW and OAE to understand how phytoplankton species respond to Ni perturbations (Bach et al., 2019).

Dissolved Ni occurs in low concentrations (2-4 nmol/L) in the sea surface, but concentrations increase with depth (up to 11 nmol/L) in the North Pacific (Bruland, 1980; Sclater et al., 1976). The depletion in the surface in some ocean regions is thought to be caused by phytoplankton utilization of dissolved Ni and the enrichment with depth due to remineralization of exported particulate Ni (Glass and Dupont, 2017; Dupont et al., 2010; Morel, 2008). The nutrient-like vertical profile of Ni indicates that it is a bioactive element for phytoplankton in some areas. Indeed, Ni is an essential co-factor for some enzymes (Zamble, et al. 2017; Sunda, 1989) and two major functions of Ni for phytoplankton metabolism have been documented. First, Ni is known to be involved in urea utilization. Urea is an ecologically important nitrogen source that can support 5-50% of oceanic primary production (Wafar et al., 1995). Most marine phytoplankton, including cyanobacteria, haptophytes, dinoflagellates, and diatoms, use the Ni-containing enzyme urease to hydrolyse urea to ammonium and CO_2 ($(NH_2)_2CO + H_2O \rightarrow CO_2 + 2NH_3$) (Holm and Sander, 1997; Dupont et al., 2010). Second, Ni can be a co-factor for the enzyme superoxide dismutase (SOD) (Wolfe-Simon et al., 2005). SOD is important for the survival of photosynthetic organisms (Glass and Dupont, 2017). The highly reactive and noxious superoxide anion radical (O_2^-) is a metabolic by-product of aerobic respiration and oxygenic photosynthesis (Fridovich, 1998). SOD can turn O_2^- into molecular oxygen (O_2) and hydrogen peroxide (H_2O_2). Since nitrogenase can be inactivated by reactive oxygen species, such as O_2^-, Ni-SOD is indirectly involved in nitrogen fixation in cyanobacteria.

This project tested the response of 11 different marine phytoplankton species to a gradient of dissolved Ni concentrations. The phytoplankton species were exposed to this gradient under the same experimental conditions. We address the following questions: (1) how do different dissolved Ni concentrations influence phytoplankton growth and photosynthetic performance? (2) will different phytoplankton species or functional groups have different Ni sensitivities?

2 Materials and Methods

Eleven axenic cultures from four different phytoplankton functional groups (diatoms, haptophytes, cyanobacteria, and dinoflagellates) were obtained from the Australian National Algae Culture Collection. We selected species from temperate regions as they can be grown at the same temperature and seawater medium. Selected species included three diatoms: *Asterionellopsis glacialis* (CS-135), *Nitzschia closterium* (CS-5), *Phaeodactylum*

https://doi.org/10.5194/bg-2021-312
Preprint. Discussion started: 3 January 2022

tricornutum (CS-29); four haptophytes: *Cricosphaera* sp. (CS-1183), *Emiliania huxleyi* (CS-1185), *Isochrysis galbana* (CS-186), *Prymnesium parvum* (CS-659); three cyanobacteria: *Geitlerinema* sp. (CS-897), *Oscillatoria* sp. (CS-52), *Synechococcus* sp. (CS-205); and one dinoflagellate *Amphidinium carterae* (CS-740).

2.1 Growing phytoplankton in artificial seawater medium

This study used Aquil medium due to its wide application in trace metal experiments (Price et al., 1989). The medium is composed of artificial seawater where Milli-Q grade water is mixed with ultra-pure salts to reproduce the major ion composition of seawater (Pausch et al., 2019). The medium was filtered through a 0.2 µm pore size filter and sterilized in a microwave for a total of 11 minutes in acid-cleaned polycarbonate bottles (2 L) (Price et al., 1989). This artificial seawater is further enriched with the elements necessary for algal growth, such as vitamins, macronutrients (nitrate (NO_3^-) = 100 µmol/L, phosphate (PO_4^{3-}) = 10 µmol/L, and silicate (SiO_3^{2-}) = 100 µmol/L), and various essential trace metals such as iron and manganese (Table A1). The trace metals were buffered with 100 µmol/L ethylenediaminetetraacetic acid (EDTA). Seventeen Aquil media were produced that differed in the amount of Ni that was added, as will be described in more detail in the next section. Media preparation was done in a trace metal clean laminar flow bench. The salinity and pH (NBS scale) of Aquil media were 35 and 8.1 respectively.

Phytoplankton species were cultivated in acid-cleaned (10% HCl for at least 24 h) polycarbonate tubes (30 mL, Nalgene ™). These polycarbonate tubes (one tray with 40 tubes) were filled with Milli-Q water and then sterilized in the microwave for 8 minutes. The Aquil media were transferred from 1 L bottles into empty polycarbonate tubes under the clean bench under the trace metal clean laminar flow bench. Phytoplankton were added to the medium once it had reached chemical equilibrium (see next section).

The cultures were grown in a light chamber at 17°C. All polycarbonate tubes were mounted onto a self-made "phytoplankton disc", which rotated at 0.8 revolutions per minute (Fig. 1 (a)). The phytoplankton disc ensured that equal light intensity was provided to all cultures and that phytoplankton cells were kept in suspension. The light was provided on a 14-to-10-hour daily cycle (cool white fluorescence light) where light intensities were 58 µmol photons m^{-2} s^{-1} (14 hours) and 23 µmol photons m^{-2} s^{-1} (10 hours). This unusual light cycle was due to some lights in the room being plugged in energy sources, which had separate light-dark cycle setups linked to the computer system at the Institute of Marine and Antarctic Studies. Initially, we were not aware of this additional cycle and only realized the issue during the experiment. Therefore, we continued with this light cycle to maintain

https://doi.org/10.5194/bg-2021-312
Preprint. Discussion started: 3 January 2022

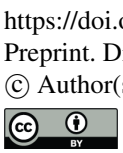

Biogeosciences Discussions Open Access EGU

comparability between experiments. However, this issue does not affect the interpretation of the results as all species and replicates received the same amount of light throughout the experiment. The light intensity was the average light intensity at each of the 88 spots on the phytoplankton disc measured with a Licor light meter.

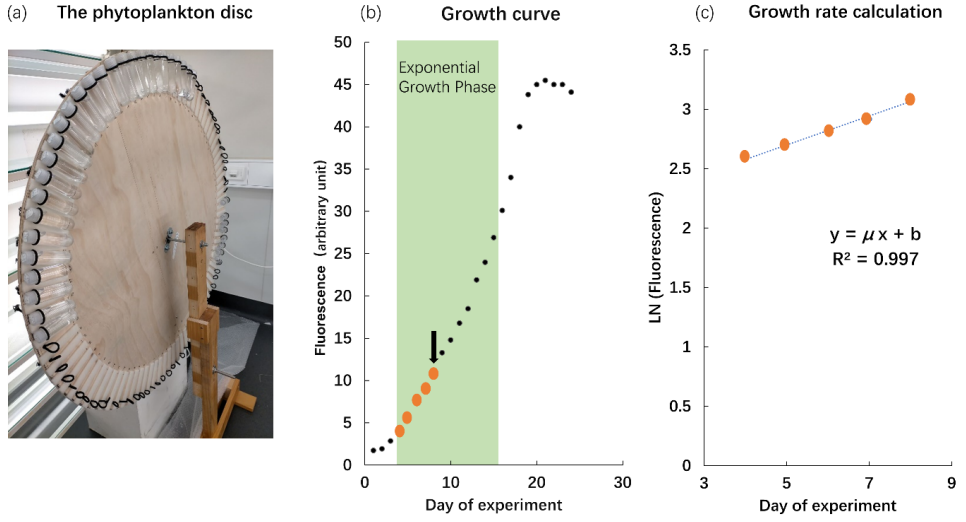

Figure 1. The phytoplankton disc and growth rate calculation. (a) The phytoplankton disc, with polycarbonate tubes mounted using elastic bands to the edge of the circular disc. The disc rotated with 0.8 revolutions per minute during the experiment. (b) In vivo chlorophyll fluorescence during the growth cycle of phytoplankton cultures. We only used fluorescence values where biomass inside the polycarbonate tubes was still relatively low (maximum up to a fluorescence of 13) as indicated in this example with the thick orange dots. The arrow indicates the time when the culture was usually transferred into the next batch of fresh medium. (Please note that the data illustrated here is from a test where we let the culture grow into nutrient depletion.) (c) The fluorescence values measured at low biomass were ln-transformed and plotted against time (day). The slope of the linear regression in this plot represents the specific growth rate (μ; d^{-1}).

2.2 Nickel treatment

Aquil media were enriched with different concentrations of $NiCl_2$: 0, 5, 10, 20, 30, 50, 70, 100, 150, 200, 300, 400, 500, 700, 1000, 10000 and 50000 nmol/L. Unless otherwise noted, "Ni concentration" refers to the total added dissolved Ni concentration. For illustration and discussion of the data, concentrations were negatively $\log_{10}$ transformed:

$$pNi = -\log_{10}(Ni) \quad \text{Eq. (1)}$$

where Ni is the total dissolved concentration of Ni in mol/L. This kind of transformation is also used to convert hydrogen ion concentrations to pH and is commonly used in studies investigating trace metal sensitivities to better

https://doi.org/10.5194/bg-2021-312
Preprint. Discussion started: 3 January 2022

visualize data when trace metal concentrations vary over orders of magnitude (Dupont et al., 2008).

Media were allowed to equilibrate chemically for at least 24 h before being inoculated with phytoplankton. To acclimate the phytoplankton strains, stock cultures were first transferred into Aquil medium without Ni enrichment. They were then cultivated for at least 3 batch cycles (i.e., transferred from one polycarbonate tube to the next one) before being transferred to polycarbonate tubes with the different Ni treatments. This ensured that the phytoplankton species were acclimated to Aquil medium before the Ni experiment commenced.

Due to the addition of the ligand EDTA to the Aquil media, the "free Ni" ion concentrations (i.e., Ni^{2+}) were substantially lower than the total dissolved Ni concentrations as was calculated with the chemical speciation software Visual MINTEQ 3.1 (Gustafsson, 2011). We were interested to see if the response of phytoplankton to Ni may be different in other growth media where no EDTA was added. Therefore, we prepared a batch of natural seawater medium with water sampled from 15 m in the Southern Ocean (58.02 °S, 141.17 °E). This natural seawater was filtered through an acid-cleaned 0.2 µm filter and sterilized in the microwave. The same amount of macro-nutrients (N, P and Si) and vitamins were added as in the Aquil medium (mentioned above). The trace metal additions to the Southern Ocean seawater (no Ni included) were adjusted to a similar free trace metal concentration (nutrient-replete) as in Aquil medium (Table A1). For the experiment with natural seawater, we set up a dissolved Ni gradient with 17 concentrations: 0, 1, 2, 5, 10, 20, 30, 50, 70, 100, 150, 200, 300, 400, 500, 700, and 1000 nmol/L. The extremely high Ni concentrations designed for the Aquil medium were avoided as we assumed the organic ligand concentrations in natural seawater to be much lower than the concentration of EDTA added in Aquil medium and therefore the concentration of free Ni^{2+} to be higher. We used *P. tricornutum* (CS-29) for this experiment. *Phaeodactylum tricornutum* was transferred from the stock cultures into natural seawater medium for 3 batches cycles prior to the experiment with different Ni treatments as described for the Aquil medium above.

The total ion concentrations of each trace metal in natural seawater and Aquil media before additions were measured using a seaFAST system and inductively-coupled plasma mass spectrometry (ICP-MS). The free ion concentrations were calculated with Visual MINTEQ 3.1 based on the total ion concentration together with the added concentration (Table 1).

https://doi.org/10.5194/bg-2021-312
Preprint. Discussion started: 3 January 2022

Table 1. The total dissolved concentrations and free ion concentrations of Ni in different media.

Aquil medium					Southern Ocean seawater medium				
Added Ni concentration (nmol/L)	Total dissolved Ni concentration (mol/L)	pNi	Free Ni^{2+} concentration (mol/L)	pNi^{2+}	Added Ni concentration (nmol/L)	Total dissolved Ni concentration (mol/L)	pNi	Free Ni^{2+} concentration (mol/L)	pNi^{2+}
0	7.1×10^{-11}	10.2	9.4×10^{-17}	16.0	0	8.6×10^{-9}	8.1	6.1×10^{-9}	8.2
5	5.1×10^{-9}	8.3	6.8×10^{-15}	14.2	1	9.6×10^{-9}	8.0	6.8×10^{-9}	8.2
10	1.0×10^{-8}	8.0	1.3×10^{-14}	13.9	2	1.1×10^{-8}	8.0	7.5×10^{-9}	8.1
20	2.0×10^{-8}	7.7	2.7×10^{-14}	13.6	5	1.4×10^{-8}	7.9	9.7×10^{-9}	8.0
30	3.0×10^{-8}	7.5	4.0×10^{-14}	13.4	10	1.9×10^{-8}	7.7	1.3×10^{-8}	7.9
50	5.0×10^{-8}	7.3	6.7×10^{-14}	13.2	20	2.9×10^{-8}	7.5	2.0×10^{-8}	7.7
70	7.0×10^{-8}	7.2	9.3×10^{-14}	13.0	30	3.9×10^{-8}	7.4	2.7×10^{-8}	7.6
100	1.0×10^{-7}	7.0	1.3×10^{-13}	12.9	50	5.9×10^{-8}	7.2	4.2×10^{-8}	7.4
150	1.5×10^{-7}	6.8	2.0×10^{-13}	12.7	70	7.9×10^{-8}	7.1	5.6×10^{-8}	7.3
200	2.0×10^{-7}	6.7	2.7×10^{-13}	12.6	100	1.1×10^{-7}	7.0	7.8×10^{-8}	7.1
300	3.0×10^{-7}	6.5	4.0×10^{-13}	12.4	150	1.6×10^{-7}	6.8	1.1×10^{-7}	7.0
400	4.0×10^{-7}	6.4	5.4×10^{-13}	12.3	200	2.1×10^{-7}	6.7	1.5×10^{-7}	6.8
500	5.0×10^{-7}	6.3	6.7×10^{-13}	12.2	300	3.1×10^{-7}	6.5	2.2×10^{-7}	6.7
700	7.0×10^{-7}	6.2	9.4×10^{-13}	12.0	400	4.1×10^{-7}	6.4	2.9×10^{-7}	6.5
1000	1.0×10^{-6}	6.0	1.4×10^{-12}	11.9	500	5.1×10^{-7}	6.3	3.6×10^{-7}	6.4
10000	1.0×10^{-5}	5.0	1.5×10^{-11}	10.8	700	7.1×10^{-7}	6.2	5.0×10^{-7}	6.3
50000	5.0×10^{-5}	4.3	1.4×10^{-10}	9.9	1000	1.0×10^{-6}	6.0	7.2×10^{-7}	6.1

2.3 Growth rate measurement

Growth rate measurements were conducted according to the methods described by Andersen (2005). Briefly, the chlorophyll fluorescence of the cells was recorded daily at the same time with a Turner Model 10-AU fluorometer. During the measurements, polycarbonate tubes did not have to be opened because they fit within the sample chamber of the fluorometer. This reduced the risk of contamination as the polycarbonate tubes remained closed throughout the experiment. Fluorescence signals of samples were measured after 20 minutes of dark acclimation. The fluorescence values were *ln*-transformed and plotted as a function of incubation days. A linear regression was fitted during the exponential phase of phytoplankton growth with the specific growth rate (μ; d^{-1}) represented by the slope of the linear regression (Fig. 1(b) and (c)). We only used fluorescence values up to 13 (arbitrary unit) for our growth rate calculations so that the biomass in the incubation bottles remained relatively low and consistent with the dilute batch culture principle (Laroche et al., 2010).

https://doi.org/10.5194/bg-2021-312
Preprint. Discussion started: 3 January 2022

Reliable estimates of exponential growth rates in dilute batch cultures require multiple serial transfers of cultures (all performed while the strain is still in exponential growth) to allow the time for cultures to acclimate to the experimental conditions (Brand et al., 1981; Andersen, 2005). Therefore, the phytoplankton species were transferred into new polycarbonate tubes containing fresh medium during their early exponential stage for 3 batch cycles prior to recording growth rates shown in the results. This meant that cultures were usually growing in their respective treatment conditions for at least three weeks.

2.4 Fast repetition rate fluorometry

We conducted photo-physiological measurements at the end of each batch cycle. A Fast repetition rate (FRR) fluorometry (Fast Ocean Sensor FRRf3, Chelsea Instruments Group) was used to measure the maximum quantum yield, F_v/F_m, and the functional absorption cross-section of photosystem II (σ_{PSII}; nm^2 reaction centre $(RC)^{-1}$). These measurements were done with cultures directly after they had been used to inoculate the subsequent batch cycle (hence avoiding contamination of ongoing cultures). Cultures were kept in dark for 20 minutes before the measurements. Phytoplankton samples were added to the FRR fluorometry cuvette, which was temperature-controlled at 17 °C. Filtered Aquil media (or natural seawater media) were used at the beginning of the measurement for blank calibration. Throughout the experiment, FRR fluorometry was used with an acquisition sequence of 100 saturation flashes for 200 µs, 40 relaxation flashes for 2.4 ms, while the flash duration was set to 100 µs (Schallenberg et al., 2020). In each acquisition sequence, three channels with different light wavelengths were used: channel A with 450 nm light; channel B with 450 nm and 530 nm light; and channel C with 450 nm and 624 nm. Due to various types of photosynthetic pigments across the phytoplankton functional groups, the FRR fluorescence results from channel A (450 nm) were used to analyse diatoms, haptophytes, and dinoflagellates photosynthetic performance, while channel C (450 nm and 624 nm) results were used to analyse the photosynthetic performance of cyanobacteria. At least 10 acquisitions were measured for each sample and used to calculate the average value of F_v/F_m and σ_{PSII}. F_v/F_m is usually lower under nutrient or light stress (summarized by Suggett et al. (2009)), while σ_{PSII} describes the ability of light to promote a photochemical reaction in PSII (Falkowski and Raven, 1997). The value of F_v/F_m and σ_{PSII} are known to vary among algal taxa (Suggett et al., 2009). Typically, cells growing in batch cultures at steady state exhibit a constant value of F_v/F_m and σ_{PSII} during exponential growth phase (Parkhill et al., 2001).

https://doi.org/10.5194/bg-2021-312
Preprint. Discussion started: 3 January 2022

2.5 Data analysis

The growth rate and photo-physiological response of phytoplankton was analysed using generalised additive models (GAMs) and plotted in RStudio (R packages "mgcv" and "ggplot2"). For the GAM analyses, we assumed that growth rates, F_v/F_m and σ_{PSII} of phytoplankton would show an optimum curve in response to the wide range of Ni concentrations: Ni limitation at the lower extremes, Ni inhibition at the upper extremes and an optimum at some intermediate Ni concentration. GAMs were fitted to plots to assess the presence of a relationship between Ni concentration, growth rates and photo-physiological responses. P-values of the smooth terms of GAM models greater than 0.05 indicated that there was no statistically significant trend in the response variable (μ, F_v/F_m or σ_{PSII}) in response to the wide Ni gradient (i.e., the smooth term was not significantly different from a horizontal line and therefore no statistically significant relationship between Ni and the measured parameter present). The general GAM equation is:

$$Y = I_0 + S\,(\mathrm{pNi}) + e \qquad \text{Eq. (2)}$$

where Y is the response variable (μ, F_v/F_m and σ_{PSII}); I_0 is the intercept; S(pNi) is the non-parametric smooth function according to pNi; and e the error. The k-value (basis dimension) of GAMs was set to the minimum k-value that fitted the curve and explained the data points without over- or under-fitting.

3 Results

3.1 Growth rates comparison

Most trace metals in seawater are partially bound by organic ligands and their bioavailable "free" concentrations are lower than the total dissolved ion concentrations (Van Den Berg and Nimmo, 1987). The thermodynamic equilibrium concentrations of the $-\log_{10}$ transformed "free Ni concentrations" (pNi^{2+}) and total dissolved Ni concentrations (pNi) in the different media (see Eq. 1 and Table 1.) correlate linearly ($R^2 > 0.99$). Thus, both can be displayed as separate x-axes on the same plot (Fig. 2, 3 and 4). In the Southern Ocean seawater media, the differences between pNi and pNi^{2+} are very small due to the assumed low concentration of ligands. In Aquil, however, these differences are large due to the presence of EDTA.

https://doi.org/10.5194/bg-2021-312
Preprint. Discussion started: 3 January 2022

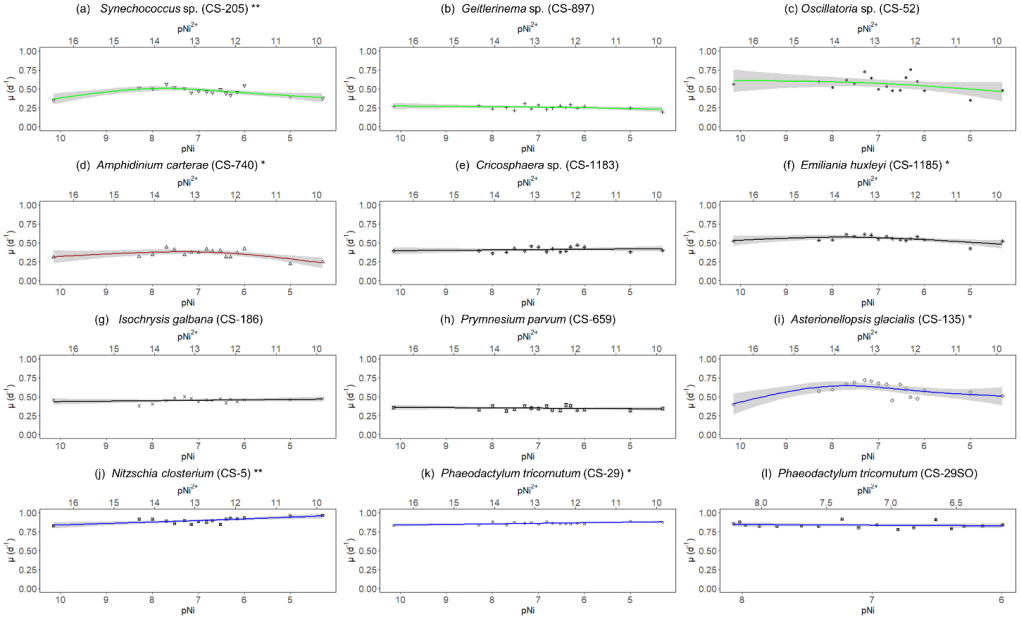

Figure 2. Growth rates of different phytoplankton strains in a large gradient of Ni concentrations. The species name is shown in each subplot with the strain number in the parentheses. pNi and pNi^{2+} are the $-\log_{10}$ transformed values of the total dissolved and free Ni concentrations, respectively (Eq. (1)). A smaller value represents a higher concentration. Plots (a)-(c) are cyanobacteria; plot (d) is a dinoflagellate; plots (e)-(h) are haptophytes; plots (i)-(l) are diatoms. Plots (a)-(k) show growth rates in Aquil media while plot (l) shows growth rates of *P. tricornutum* in natural seawater media. Solid lines represent the smooth terms produced from GAMs using the growth rate data and pNi concentrations. Shading indicates the 95% confidence interval. P-values <0.05 indicate that the smooth term is significantly different from a straight horizontal line. P-values <0.05 are indicated by an *, and P-values <0.01 are indicated by **.

Every strain was able to grow in all Ni concentrations in Aquil media for at least 3 batch cycles. In general, Ni had limited impact on phytoplankton growth rates in the tested range. Six out of the 11 strains displayed statistically significant growth rate changes in response to Ni sensitivity (Fig. 2, Table 2). These strains were *Synechococcus* sp. (CS-205), *A. carterae* (CS-740), *E. huxleyi* (CS-1185), *A. glacialis* (CS-135), *N. closterium* (CS-5), and *P. tricornutum* (CS-29). Among these strains, *N. closterium* (CS-5) and *P. tricornutum* (CS-29) had consistent increasing growth rates when pNi increased (Fig. 2 (j) and (k)). Other strains displayed optimum curves response patterns, although variations in growth rates between the low, high, and optimum concentration of pNi and these trends were mostly small. Most of their optimal growth rates were in the range of pNi 8-7 (10 nmol/L to 100 nmol/L). Growth rates of the other strains (*Geitlerinema* sp. (CS-897), *Oscillatoria* sp. (CS-52), *Cricosphaera* sp. (CS-1183), *I. galbana* (CS-186), and *P. parvum* (CS-659)) were unaffected by different Ni concentrations.

https://doi.org/10.5194/bg-2021-312
Preprint. Discussion started: 3 January 2022

Table 2. Approximate significance of the smooth terms for GAMs. Three separate GAMs were used to calculate the impacts of pNi on μ, F_v/F_m and σ_{PSII} (Eq. 2). P-values <0.05 indicate that the smooth term is significantly different from a straight line. P-values <0.05 are indicated by an *, and P-values <0.01 are indicated by **. Adj r^2 is the adjusted r squared value. DE stands for deviance explained.

Strain number	Strain name	P-value of μ		Adj r^2	DE	P-value of F_v/F_m		Adj r^2	DE	P-value of σ_{PSII}		Adj r^2	DE
CS-205	*Synechococcus* sp.	0.005	**	0.554	0.628	0.003	**	0.515	0.574	0.508		-0.035	0.030
CS-897	*Geitlerinema* sp.	0.313		0.086	0.168	0.003	**	0.528	0.585	0.173		0.156	0.235
CS-52	*Oscillatoria* sp.	0.282		0.099	0.184	0.114		0.102	0.158	0.068		0.262	0.347
CS-740	*Amphidinium carterae*	0.019	*	0.433	0.518	0.030	*	0.228	0.276	0.000	**	0.783	0.822
CS-1183	*Cricosphaera* sp.	0.504		-0.034	0.030	0.574		-0.044	0.022	0.287		0.104	0.198
CS-1185	*Emiliania huxleyi*	0.048	*	0.342	0.434	0.588		-0.045	0.020	0.178		0.251	0.380
CS-186	*Isochrysis galbana*	0.347		-0.004	0.059	0.697		-0.056	0.010	0.763		-0.026	0.058
CS-659	*Prymnesium parvum*	0.510		-0.035	0.030	0.348		-0.004	0.059	0.003	**	0.519	0.577
CS-135	*Asterionellopsis glacialis*	0.034	*	0.418	0.512	0.080		0.246	0.332	0.006	**	0.528	0.601
CS-5	*Nitzschia closterium*	0.004	**	0.459	0.500	0.120		0.097	0.153	0.328		0.001	0.064
CS-29	*Phaeodactylum tricornutum*	0.013	*	0.300	0.344	0.389		0.066	0.157	0.025	*	0.356	0.432
CS-29SO	*Phaeodactylum tricornutum*	0.517		-0.036	0.029	0.662		-0.018	0.062	0.260		0.117	0.208

The cyanobacterium *Oscillatoria* sp. (CS-52) tended to aggregate during culturing and the fluorescence signals were more variable on a day-to-day basis. This made the growth rate calculation less accurate, indicated by lower R^2 values in linear regression when fitting ln-transformed data over time to calculate the growth rate.

We were interested if we could trust singular datapoints at the extreme ends of the optimum curves, as they often drove trends in our data (e.g., *Synechococcus* in Fig. 2 at pNi <7.5, total dissolved Ni < 30 nmol/L). Therefore, we did an additional experiment with *Synechococcus* sp. (CS-205) where we replicated the lowest added Ni treatment (0 nmol/L; 0.07 nmol/L including background Ni) and the optimum Ni concentration (20 nmol/L) (Table 3). The results confirmed the trend in the optimum curve, with the added 20 nmol/L Ni resulting in significantly enhanced growth rates (Table 3).

https://doi.org/10.5194/bg-2021-312
Preprint. Discussion started: 3 January 2022

Table 3. Physiological responses of *Synechococcus* sp. (CS-205) at two different Ni concentrations with 3 replicates each treatment (shown individually). Ni con. is the total dissolved Ni concentration in the media. μ means growth rate (day^{-1}). SD means standard deviation. P-value was calculated using T-test. The unit of σ_{PSII} is nm^2 reaction centre $(RC)^{-1}$.

Ni con. (nmol/L)	μ	Average μ	SD	P-value of μ	Fv/Fm	Average Fv/Fm	SD	P-value of Fv/Fm	σ_{PSII}	Average σ_{PSII}	SD	P-value of σ_{PSII}
0	0.25				0.33				228			
0	0.31	0.30	0.04		0.34	0.35	0.02		236	230	6.23	
0	0.33			0.001	0.37			0.179	224			0.797
20	0.54				0.41				227		21.6	
20	0.51	0.52	0.03		0.41	0.38	0.04		247	226		
20	0.49				0.34				204			

3.2 Photosynthesis performance of phytoplankton

The FRR fluorescence data were largely consistent with the growth rate data in that no strong trends within the Ni range tested were observed for most of species. The σ_{PSII} and F_v/F_m measurements across the Ni gradient revealed minimal trends, with generally little variation between treatments (Fig. 3 and 4). A few exceptions to this general pattern results are mentioned below.

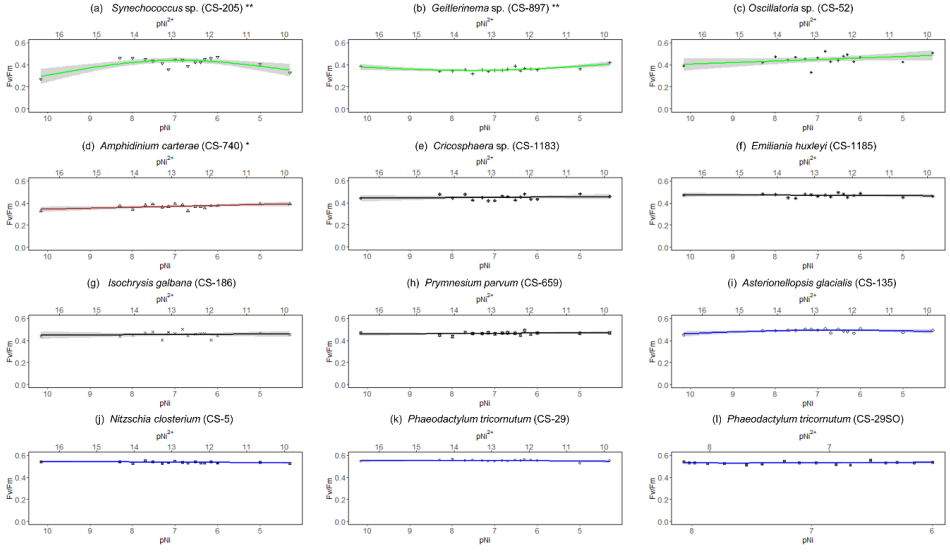

https://doi.org/10.5194/bg-2021-312
Preprint. Discussion started: 3 January 2022

Biogeosciences
Discussions
Open Access
EGU

Figure 3. F_v/F_m results of phytoplankton cultures. pNi and pNi^{2+} are the -log_{10} transformed values of the total dissolved and free Ni^{2+} concentrations (Eq. (1)). A smaller value represents a higher concentration. Plots (a)-(c) are cyanobacteria; the plot (d) is a dinoflagellate; plots (e)-(h) are haptophytes; plots (i)-(l) are diatoms. Plots (a)-(k) were from strains growing in Aquil media while plot (l) are results for *P. tricornutum* growing in natural seawater media. Solid lines represent the smooth terms produced from GAMs using the growth rate data and pNi concentrations. Shading indicates the 95% confidence interval. P-values <0.05, indicate that the smooth term is significantly different from a straight line. P-values <0.05 are indicated by an *, and P-values <0.01 are indicated by **.

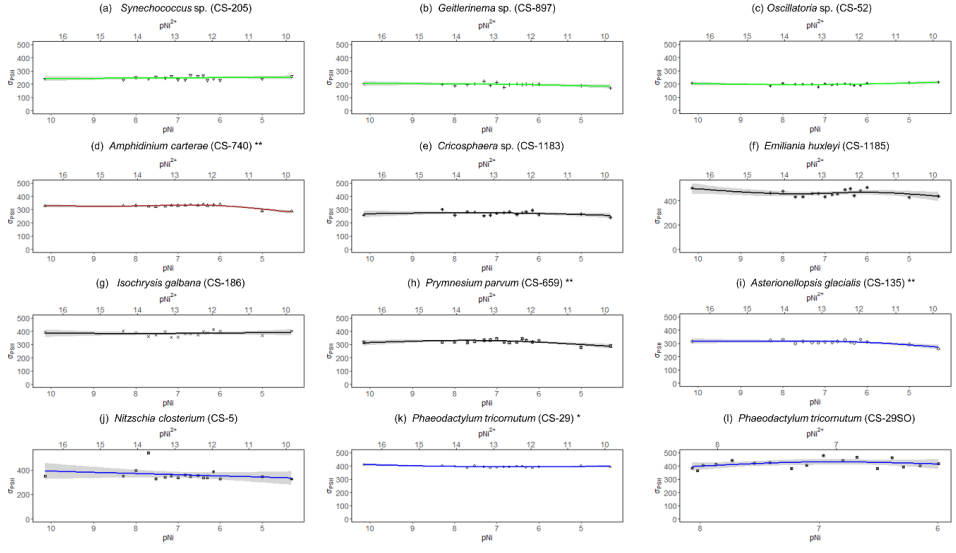

Figure 4. σ_{PSII} results of phytoplankton cultures. pNi and pNi^{2+} are the -log_{10} transformed values of the total dissolved and free Ni^{2+} concentrations (Eq. (1)). A smaller value represents a higher concentration. The unit of σPSII is nm^2 reaction centre $(RC)^{-1}$. Plots (a)-(c) are cyanobacteria; the plot (d) is a dinoflagellate; plots (e)-(h) are haptophytes; plots (i)-(l) are diatoms. Plots (a)-(k) were from strains growing in Aquil media while plot (l) are results for *P. tricornutum* growing in natural seawater media. Solid lines represent the smooth terms produced from GAM models using the growth rate data and pNi concentrations. Shading indicates the 95% confidence interval. P-values <0.05, indicate that the smooth term is significantly different from a straight line. P-values <0.05 are indicated by an *, and P-values <0.01 are indicated by **.

Synechococcus sp. (CS-205) had higher F_v/F_m values in the mid-pNi range (pNi 8-6, 10-1000 nmol/L) and the lowest F_v/F_m value was in the Aquil medium without any Ni addition. In contrast, *Geitlerinema* sp. (CS-897) had lower F_v/F_m values in the mid-pNi range but the variation between maximum and minimum F_v/F_m values was small. These two strains, however, exhibited little change in σ_{PSII} over the range of Ni treatment. Some species (e.g., *A. carterae* (CS-740), *P. parvum* (CS-659) and *A. glacialis* (CS-135)) had slightly lower σ_{PSII} values at the highest Ni concentrations (>10000 nM) suggesting some reduction in light harvesting capacity at high Ni

https://doi.org/10.5194/bg-2021-312
Preprint. Discussion started: 3 January 2022

concentrations. The small P-value of the smooth terms (Table 2) are likely driven by these low σ_{PSII} values in the high Ni concentrations. In general, most of the tested strains appeared photosynthetically healthy across the tested Ni gradient.

The most pronounced effect of Ni was observed in F_v/F_m for *Synechococcus* sp. (Fig. 3). F_v/F_m was considerably lower at pNi=10.2 (0.07 nmol/L) than at the optimum concentrations (approximately pNi=7.7, 20 nmol/L). Our additional experiment with *Synechococcus*, where we replicated the pNi 10.2 and 7.7 treatments three times, did not confirm this trend (Table 3). Neither F_v/F_m nor σ_{PSII} values were significantly different between the two Ni concentrations (Table 3).

3.3 Comparison between Aquil media and the natural seawater media

Like in Aquil media, *P. tricornutum* (CS-29) growing in the natural Southern Ocean seawater media showed no significant trend (F_v/F_m) or particularly strong changes (growth rate, σ_{PSII}) across the experimental Ni concentration gradient. The average growth rate of 0.8 d^{-1} was almost the same as the growth rates of the cultures growing in Aquil media (Fig. 2 (k)) and absolute numbers were also very similar for the σ_{PSII} and F_v/F_m data (Fig. 3 and 4).

4 Discussion

4.1 Phytoplankton sensitivities to different Ni concentrations

Based on growth rates and FRR fluorescence results, we conclude that changes in dissolved Ni, within the range tested and under the experimental conditions, do not have a strong effect on the 11 phytoplankton species. Only a few species showed significant trends in growth rates and/or photophysiological parameters and most of these trends were not very pronounced. An exception was *Synechococcus* sp. (CS-205), which showed a significant and quite pronounced growth rate enhancement of 74% from the lowest to optimum Ni (20 nmol/L) and then gradually declining growth rates towards the highest Ni. Likewise, growth rates of *A. carterae* (CS-740) showed a relatively pronounced Ni-sensitivity, following an optimum curve with highest growth rates between a pNi of 8-7 (10-100 nmol/L). The Ni sensitivity of growth rates in the other species where significant trends were detected were smaller. However, we emphasise that even a small difference in growth rate can have a pronounced effect on population sizes during extended periods of growth due to the exponential nature of phytoplankton reproduction. For example,

https://doi.org/10.5194/bg-2021-312
Preprint. Discussion started: 3 January 2022

an increase of growth rate by 0.05 d^{-1} (as frequently observed in our data; Fig. 2) would lead to a ~65% larger population at the end of a 10-day growth period. Furthermore, even if a species is completely insensitive to Ni it may still be affected indirectly within a competitive environment with multiple phytoplankton species present. This is because other species may benefit from, or be inhibited by, changing Ni concentration thereby altering the competition for nutrient resources. Therefore, small changes in growth rates should not be readily marginalised as they may still be of ecological and biogeochemical relevance.

The inhibition of growth rate or photosynthesis performance was evident in a few species when pNi reached 5 (10000 nmol/L) (i.e., Fig. 2(a) and (d)), but most species did not have growth inhibition in high Ni concentration. The relatively small effects of high Ni on growth rates, F_v/F_m and σ_{PSII} were surprising because we expected stronger species-dependent Ni sensitivity within the pNi range of 9-5, at least based on the available experimental evidence summarized by Glass and Dupont (2017). There are several potential reasons for the disagreement on the Ni sensitivity results from previous research. These will be discussed in the following subsections.

4.1.1 Dependency of Ni sensitivity on nitrogen sources

It has been reported that phytoplankton species have different Ni sensitivities depending on the nitrogen (N) source supporting growth. Oliveira and Antia (1986) found that 9 out of 12 phytoplankton species tested in their experiments showed faster growth when urea-enriched growth medium was supplemented with Ni. In contrast, no or less benefit of Ni was observed when the same species were grown in nitrate-enriched medium. Very similar observations of a growth-enhancing effect of Ni only when urea is the N source was later made by Price and Morel (1991) and Egleston and Morel (2008) in experiments with two diatom (*Thalassiosira*) species. Based on these previous findings we conclude that the generally limited sensitivities observed in our study are partially due to the chosen N source.

In oceans, nitrate fuels large parts of new primary production, i.e., production based on allochthonous nitrogen inputs to the euphotic zone (Eppley and Peterson, 1979). For example, nitrate is a key N source for new primary production in upwelling regions such as the Southern Ocean (Maccready and Quay, 2001) and Eastern Boundary Upwelling Systems (Messié et al., 2009). It is also mixed into the surface during winter mixing and therefore important for new production during the phytoplankton spring bloom in temperate regions (Sieracki et al., 1993). Although the role of urea in marine primary production is less studied than the role of nitrate and ammonium, it likely plays an important role (Wafar et al., 1995). Like nitrate, urea can also be of allochthonous origin and

https://doi.org/10.5194/bg-2021-312
Preprint. Discussion started: 3 January 2022

therefore by definition support new primary production. This is likely to occur in coastal regions where urea runoff from land, amplified by sewage effluents and agricultural activities, can be significant (Glibert et al., 2006). Urea is also produced during heterotrophic mineralization (Glibert et al., 2006), therefore constituting a predominant source for regenerated primary production – i.e., production based on remineralized nutrient sources (Eppley and Peterson, 1979). Indeed, ship-board enrichment experiments in the North Pacific have shown that urea strongly enhances phytoplankton growth, especially growth of the cyanobacterium *Prochlorococcus* (Shilova et al., 2017). We therefore conclude that the wide-spread relevance of urea for phytoplankton growth, and the dependence of urea cycling on Ni, suggests that Ni-sensitivities of many phytoplankton species may be more pronounced in real-world conditions than our simplified laboratory experiments would suggest.

4.1.2 Dependency of Ni sensitivity on organic ligand concentration

Organic ligands can chelate dissolved trace metals thereby changing their chemical speciation (Van Den Berg and Nimmo, 1987). It is currently not known what chemical species of dissolved Ni influence phytoplankton physiology. If phytoplankton can access the total dissolved Ni pool, then experiments with different ligand concentrations could be more easily compared. However, most research suggests that phytoplankton are not primarily sensitive to the total dissolved Ni concentration but interact with free Ni^{2+} ions (Dupont et al., 2010; Hudson and Morel, 1993; Morel et al., 1991). Free Ni^{2+} only constitutes a fraction of the total dissolved Ni concentration depending on the organic ligand concentration (Donat et al., 1994). Unfortunately, ligands are chemically diverse and difficult to measure, meaning that their influence may not always be accounted for, and comparability between studies is difficult.

Our culture medium (Aquil) contained 100 µmol/L EDTA. Thus, despite dissolved Ni concentrations up to 50 µmol/L, free Ni^{2+} concentrations were maximally 0.14 nmol/L. These concentrations will be lower than in other studies where comparable amounts of total Ni, but less EDTA was added. In natural seawater, organic ligands concentrations vary widely between regions. In regions with relatively high ligand concentrations, such as freshwater, 99.9% of dissolved Ni can be complexed (Xue et al., 2001). In seawater, generally 10%-50% of the total dissolved Ni is complexed by ligands depending on the region (Achterberg and Van Den Berg, 1997; Donat et al., 1994; Byrne, 2003; Saito et al., 2004).

The current understanding of organic complexation of Ni in surface seawater suggests that free Ni^{2+} ion concentrations are generally not orders of magnitude lower than total dissolved Ni. For example, considering that

https://doi.org/10.5194/bg-2021-312
Preprint. Discussion started: 3 January 2022

most surface seawater has a total Ni concentration of 2-10 nmol/L, free Ni^{2+} should approximately be within ~1-9 nmol/L based on the 10%-50% complexation in seawater mentioned above. These free Ni^{2+} concentrations are considerably higher than the highest free Ni^{2+} in our experiments (0.14 nmol/L), which raises the question if our experimental setup was suitable to test the influence of high Ni on phytoplankton. Answering this question is difficult as it is uncertain if total dissolved Ni concentrations influence phytoplankton physiology or only free Ni^{2+} does. Our observation of decreasing growth rates in some of the phytoplankton species in the high Ni concentrations may be seen as a hint that dissolved Ni concentrations do play a role as it seems unlikely that the marginal increases in free Ni^{2+} would induce Ni inhibition. Likewise, the almost identical growth responses to Ni of *Phaeodactylum* grown in Aquil (with high EDTA ligand concentration) and natural Southern Ocean seawater (with presumably much lower ligand concentrations) could suggest that not only free Ni^{2+} is important. Either way, these observations underscore the importance of organic ligands when studying Ni sensitivity of phytoplankton.

4.1.3 Species-specific Ni sensitivity linked to enzyme requirements

Our results are consistent with earlier studies showing that different phytoplankton species have different Ni-sensitivities (e.g., Glass and Dupont, 2017). Species-specific sensitivities can be due to the different role of Ni as a co-factor for the enzyme SOD, which catalyses the conversion of O_2^- to O_2 and H_2O_2. There are different kinds of SODs, with differing trace metal co-factor requirements. Typically, cyanobacteria utilize either Ni-SOD alone or combinations of manganese (Mn)- and Ni-SOD or iron (Fe-) and Mn-SOD. Diatoms and rhodophytes retain an active Mn-SOD, whereas chlorophytes, haptophytes, and embryophytes have either Fe-SOD or multiple combinations of Fe, Mn, and copper-zinc SODs (Wolfe-Simon et al., 2005). Ho (2013) has shown that Ni depletion limits Ni-SOD synthesis and nitrogen fixation rates in *Trichodesmium*. Moreover, Ni-SOD may be involved in the protection of the nitrogenase enzyme from superoxide inhibition during photosynthesis (Ho, 2013). Compared with other phytoplankton functional groups, cyanobacteria seem to rely more than other species on Ni-SOD which may explain their relatively high Ni-sensitivity (Dupont et al., 2008; Ho, 2013).

4.2 Implications for the assessment of ocean alkalinity enhancement

OAE can be achieved by distributing pulverized rocks on land and ocean surfaces, thereby accelerating chemical weathering rates and the generation of alkalinity. The environmental perturbation depends on the chemical

https://doi.org/10.5194/bg-2021-312
Preprint. Discussion started: 3 January 2022

composition of the applied rock minerals. If dunite is used as the source rock for OAE (an olivine-rich ultrabasic rock, often associated with vulcanism), the Ni perturbation could be particularly high as dissolution experiments with olivine powder found roughly a 3 µmol/kg increase in dissolved Ni for a ~100 µmol/kg increase in alkalinity within approximately 50 days (Montserrat et al., 2017). However, it is difficult to estimate how the free Ni^{2+} concentration will change, because it depends on the organic ligand concentration at the perturbation site. Furthermore, the optimal Ni concentration can vary considerably between phytoplankton species and as discussed above, can depend on the availability of N sources in the environment. Therefore, we need to consider not only the total inputs of Ni, but also regional differences in organic ligand concentrations, nutrient availability, and phytoplankton community composition to evaluate the potential impact of Ni on phytoplankton.

Our results suggest that excess Ni has a limited toxic impact on most of the phytoplankton species tested in our study. As the tested species cover a relatively wide range of taxa, it may be assumed that our findings can be generalised more widely to natural communities of phytoplankton. However, great care must be taken when interpreting our results because we used EDTA, a strong organic ligand, in our experiments. EDTA binds large amounts of Ni so that using the total dissolved Ni concentration for inferring the absence of a toxic effect of high Ni on phytoplankton may not be valid. Although we confirmed the absence of a toxicity effect of Ni on *P. tricornutum* (CS-29) grown in Southern Ocean seawater media (which did not contain EDTA), we cannot rule out toxicity for all the other species tested here. Because *P. tricornutum* is a known "lab rat" that readily grows under a wide range of conditions, the absence of a toxicity effect in this species is not necessarily indicative of other species. Thus, we must emphasize that our results do not reject the possibility that high Ni concentrations invoked by OAE could inhibit the growth of phytoplankton.

A potential dependency of Ni impacts on organic ligands raises the question: could such a dependency be exploited for OAE implementation strategies? As we discussed in section 4.1, open ocean ecosystems probably have lower organic ligand concentrations than many coastal or estuarine regions. Thus, a perturbation with Ni due to OAE would likely lead to a more pronounced increase in Ni^{2+} in open ocean systems than the same perturbation in a coastal/estuarine region rich in organic ligands. Therefore, regional differences in ligand concentration may be utilized to identify suitable spots for OAE applications with Ni-rich minerals, as they may reduce the environmental impact of Ni due to reduced bioavailability. It could also be argued to purposefully add ligands to seawater to reduce bioavailable Ni, but this would also reduce the availability of other, often limiting, trace metals such as iron and may therefore be unsustainable. In any case, we suggest that the impacts of Ni and other trace

https://doi.org/10.5194/bg-2021-312
Preprint. Discussion started: 3 January 2022

metals associated with minerals considered for OAE should take regional differences of organic ligand concentrations into consideration.

5 Conclusion

The Ni sensitivity of phytoplankton varied between the 11 species tested within this study but was generally rather low. This may be partly due to the use of nitrate as a nitrogen source in our experiments as other studies have revealed higher Ni sensitivities when growth is fuelled by other nitrogen-sources, such as urea. The reduced sensitivity observed in our study may also be due to the use of the high concentration of organic ligand (EDTA) added to our media, which complexed Ni making it less available for biological interactions. Considering the nitrogen sources, ligand concentration, and phytoplankton composition in test regions is important in assessing the potential environment risks of OAE. Applications of OAE with Ni-rich minerals may be safer in regions with high organic ligand concentrations and low urea concentrations, as this may reduce the impact of Ni on phytoplankton communities.

Appendix A

Table A1. The bioactive concentration of trace metals in different media calculated with Visual MINTEQ. Total ion concentrations of each trace metals from the original natural seawater and Aquil media were measured using seaFAST system. The free ion concentrations were calculated based on the total ion concentrations together with the added concentration. Temperature =17°C; pH 8.1; Ionic strength = 0.7.

	Aquil medium with 100 µmol/L EDTA	no EDTA Southern Ocean seawater medium
Metal	Free ion concentration (mol/L)	Free ion concentration (mol/L)
Se	9.43×10^{-9}	9.43×10^{-9}
Co	7.01×10^{-12}	7.48×10^{-11}
Zn	1.54×10^{-11}	5.48×10^{-10}
Cu	1.08×10^{-14}	8.33×10^{-11}
Mn	2.09×10^{-8}	6.25×10^{-9}
Fe	5.41×10^{-20}	6.68×10^{-19}

Author contributions

LTB, RS, AW, and JAG designed the experiments and JAG carried them out. LTB, RS and AW supervised the study. AF and JAG conducted GAMs analysis. JAG prepared the manuscript with contributions from all authors.

https://doi.org/10.5194/bg-2021-312
Preprint. Discussion started: 3 January 2022

Competing interests

The authors declare that they have no conflict of interest.

Data availability

Data is available in Institute for Marine and Antarctic Studies (IMAS) data catalogue, University of Tasmania (UTAS). Guo, J.: Growth rate and Fast Repetition Rate fluorometry (FRRf) of phytoplankton [Data set], IMAS, https://doi.org/10.25959/1Z63-7555, 2021.

Acknowledgements

The authors thank Pam Quayle and Axel Durand for their assistance with the experimental infrastructure.

Financial support

This study was funded by the Australian Research Council by Future Fellowship FT200100846 awarded to LTB.

References

Achterberg, E. P. and Van Den Berg, C. M. G.: Chemical speciation of chromium and nickel in the western Mediterranean, Deep-Sea Res. Pt. II , 44, 693-720, https://doi.org/10.1016/s0967-0645(96)00086-0, 1997.

Andersen, R. A., Andersen, R. A. (Ed.): Algal Culturing Techniques, Elsevier 2005.

Archer, D., Eby, M., Brovkin, V., Ridgwell, A., Cao, L., Mikolajewicz, U., Caldeira, K., Matsumoto, K., Munhoven, G., Montenegro, A., and Tokos, K.: Atmospheric lifetime of fossil fuel carbon dioxide, Annu. Rev. Earth Pl. Sc., 37, 117-134, https://doi.org/10.1146/annurev.earth.031208.100206, 2009.

Bach, L. T., Gill, S. J., Rickaby, R. E. M., Gore, S., and Renforth, P.: CO_2 removal with enhanced weathering and ocean alkalinity enhancement: potential risks and co-benefits for marine pelagic ecosystems, Front. Clim., 1, 1-21, https://doi.org/10.3389/fclim.2019.00007, 2019.

Brand, L. E., Guillard, R. R., and Murphy, L. S.: A method for the rapid and precise determination of acclimated phytoplankton reproduction rates, J. Plankton Res., 3, 193-201, https://doi.org/10.1093/plankt/3.2.193, 1981.

Bruland, K. W.: Oceanographic distributions of cadmium, zinc, nickel, and copper in the North Pacific, Earth Planet Sc. Lett., 47, 176-198, https://doi.org/10.1016/0012-821x(80)90035-7, 1980.

Byrne, R. H.: Inorganic speciation of dissolved elements in seawater: the influence of pH on concentration ratios, Geochem. T., 3, 11-16, https://doi.org/10.1039/b109732f, 2003.

Donat, J. R., Lao, K. A., and Bruland, K. W.: Speciation of dissolved copper and nickel in South San Francisco Bay: a multi-method approach, Anal. Chim. Acta., 284, 547-571, 1994.

Dupont, C. L., Barbeau, K., and Palenik, B.: Ni uptake and limitation in marine *Synechococcus* strains, Appl. Environ. Microb., 74, 23-31, https://doi.org/10.1128/AEM.01007-07, 2008.

Dupont, C. L., Buck, K. N., Palenik, B., and Barbeau, K.: Nickel utilization in phytoplankton assemblages from contrasting oceanic regimes, Deep-Sea Res. Pt. II , 57, 553-566, https://doi.org/10.1016/j.dsr.2009.12.014, 2010.

Egleston, E. S. and Morel, F. M. M.: Nickel limitation and zinc toxicity in a urea-grown diatom, Limnol. Oceanogr., 53, 2462-2471, https://doi.org/10.4319/lo.2008.53.6.2462, 2008.

https://doi.org/10.5194/bg-2021-312
Preprint. Discussion started: 3 January 2022

Eppley, R. W. and Peterson, B. J.: Particulate organic matter flux and planktonic new production in the deep ocean, Nature, 282, 677-680, https://doi.org/10.1038/282677a0, 1979.

Falkowski, P. G. and Raven, J. A.: Aquatic Photosynthesis Blackwell Science, Malden, Massachussetts, 375, 1997.

Fridovich, I.: Oxygen toxicity: a radical explanation, J. Exp. Biol., 201, 1203-1209, https://doi.org/10.1242/jeb.201.8.1203, 1998.

Friedlingstein, P., O'Sullivan, M., Jones, M. W., Andrew, R. M., Hauck, J., Olsen, A., Peters, G. P., Peters, W., Pongratz, J., Sitch, S., Le Quéré, C., Canadell, J. G., Ciais, P., Jackson, R. B., Alin, S., Aragão, L. E. O. C., Arneth, A., Arora, V., Bates, N. R., Becker, M., Benoit-Cattin, A., Bittig, H. C., Bopp, L., Bultan, S., Chandra, N., Chevallier, F., Chini, L. P., Evans, W., Florentie, L., Forster, P. M., Gasser, T., Gehlen, M., Gilfillan, D., Gkritzalis, T., Gregor, L., Gruber, N., Harris, I., Hartung, K., Haverd, V., Houghton, R. A., Ilyina, T., Jain, A. K., Joetzjer, E., Kadono, K., Kato, E., Kitidis, V., Korsbakken, J. I., Landschützer, P., Lefèvre, N., Lenton, A., Lienert, S., Liu, Z., Lombardozzi, D., Marland, G., Metzl, N., Munro, D. R., Nabel, J. E. M. S., Nakaoka, S.-I., Niwa, Y., O'Brien, K., Ono, T., Palmer, P. I., Pierrot, D., Poulter, B., Resplandy, L., Robertson, E., Rödenbeck, C., Schwinger, J., Séférian, R., Skjelvan, I., Smith, A. J. P., Sutton, A. J., Tanhua, T., Tans, P. P., Tian, H., Tilbrook, B., Van Der Werf, G., Vuichard, N., Walker, A. P., Wanninkhof, R., Watson, A. J., Willis, D., Wiltshire, A. J., Yuan, W., Yue, X., and Zaehle, S.: Global carbon budget 2020, Earth Syst. Sci. Data, 12, 3269-3340, https://doi.org/10.5194/essd-12-3269-2020, 2020.

Glass, J. B. and Dupont, C. L.: Oceanic nickel biogeochemistry and the evolution of nickel use, in: The Biological Chemistry of Nickel, edited by: Deborah Zamble, M. R.-Ż. a. H. K., Royal Society of Chemistry, United Kingdom, 12-26, 2017.

Glibert, P. M., Harrison, J., Heil, C., and Seitzinger, S.: Escalating worldwide use of urea – a global change contributing to coastal eutrophication, Biogeochemistry, 77, 441-463, http://doi.org/10.1007/s10533-005-3070-5, 2006.

Gustafsson, J. P.: Visual MINTEQ 3.0 user guide, KTH, Department of Land and Water Recources, Stockholm, Sweden, 2011.

Hartmann, J., West, A. J., Renforth, P., Köhler, P., De La Rocha, C. L., Wolf-Gladrow, D. A., Dürr, H. H., and Scheffran, J.: Enhanced chemical weathering as a geoengineering strategy to reduce atmospheric carbon dioxide, supply nutrients, and mitigate ocean acidification, Rev. Geophys., 51, 113-149, http://doi.org/10.1002/rog.20004, 2013.

Ho, T.-Y.: Nickel limitation of nitrogen fixation in *Trichodesmium*, Limnol. Oceanogr., 58, 112-120, https://doi.org/10.4319/lo.2013.58.1.0112, 2013.

Holm, L. and Sander, C.: An evolutionary treasure: unification of a broad set of amidohydrolases related to urease, Proteins, 28, 72-82, https://doi.org/10.1002/(SICI)1097-0134(199705)28:1<72::AID-PROT7>3.0.CO;2-L, 1997.

Hudson, R. J. M. and Morel, F. M. M.: Trace metal transport by marine microorganisms: implications of metal coordination kinetics, Deep-Sea Res. Pt. I., 40, 129-150, https://doi.org/10.1016/0967-0637(93)90057-A, 1993.

Ilyina, T., Wolf-Gladrow, D., Munhoven, G., and Heinze, C.: Assessing the potential of calcium-based artificial ocean alkalinization to mitigate rising atmospheric CO_2 and ocean acidification, Geophys. Res. Lett., 40, 5909-5914, https://doi.org/10.1002/2013gl057981, 2013.

IPCC: Climate Change and Land: an IPCC special report on climate change, desertification, land degradation, sustainable land management, food security, and greenhouse gas fluxes in terrestrial ecosystems, edited by Shukla P.R., Skea J., Calvo Buendia E., Masson-Delmotte V., Pörtner H.-O., Roberts D. C., Zhai P., Slade R., Connors S., Diemen R., Ferrat M., Haughey E., Luz S., Neogi S., Pathak M., Petzold J., Portugal P. J., Vyas P., Huntley E., Kissick K., Belkacemi M., Malley J., In press, 2019.

Kheshgi, H. S.: Sequestering atmospheric carbon dioxide by increasing ocean alkalinity, Energy, 20, 915-922,

https://doi.org/10.5194/bg-2021-312
Preprint. Discussion started: 3 January 2022

https://doi.org/10.1016/0360-5442(95)00035-F, 1995.

Kohler, P., Hartmann, J., and Wolf-Gladrow, D. A.: Geoengineering potential of artificially enhanced silicate weathering of olivine, P. Natl. A. Sci. USA., 107, 20228-20233, https://doi.org/10.1073/pnas.1000545107, 2010.

LaRoche, J., Rost, B., and Engel, A.: Bioassays, batch culture and chemostat experimentation, in: Guide to Best Practices for Ocean Acidification Research and Data Reporting, edited by: Riebesell, U., Fabry, V. J., Hansson, L., and Gattuso, J.P., Publications office of the European Union, 81-94, 2010.

Lenton, A., Matear, R. J., Keller, D. P., Scott, V., and Vaughan, N. E.: Assessing carbon dioxide removal through global and regional ocean alkalinization under high and low emission pathways, Earth Syst. Dynam., 9, 339-357, https://doi.org/10.5194/esd-9-339-2018, 2018.

MacCready, P. and Quay, P.: Biological export flux in the Southern Ocean estimated from a climatological nitrate budget, Deep-Sea Res. Pt. II, 48, 4299-4322, https://doi.org/10.1016/S0967-0645(01)00090-X, 2001.

Messié, M., Ledesma, J., Kolber, D. D., Michisaki, R. P., Foley, D. G., and Chavez, F. P.: Potential new production estimates in four eastern boundary upwelling ecosystems, Prog. Oceanogr., 83, 151-158, https://doi.org/10.1016/j.pocean.2009.07.018, 2009.

Montserrat, F., Renforth, P., Hartmann, J., Leermakers, M., Knops, P., and Meysman, F. J. R.: Olivine dissolution in seawater: implications for CO_2 sequestration through enhanced weathering in coastal environments, Environ. Sci. Technol., 51, 3960-3972, https://doi.org/10.1021/acs.est.6b05942, 2017.

Morel, F. M. M.: The co-evolution of phytoplankton and trace element cycles in the oceans, Geobiology, 6, 318-324, https://doi.org/10.1111/j.1472-4669.2008.00144.x, 2008.

Morel, F. M. M., Hudson, R. J. M., and Price, N. M.: Limitation of productivity by trace metals in the sea, Limnol. Oceanogr., 36, 1742-1755, 10.4319/lo.1991.36.8.1742, 1991.

Oliveira, L. and Antia, N. J.: Nickel ion requirements for autotrophic growth of several marine microalgae with urea serving as nitrogen source, Can. J. Fish. Aquat. Sci., 43, 2427-2433, https://doi.org/10.1139/f86-301, 1986.

Parkhill, J.-P., Maillet, G., and Cullen, J. J.: Fluorescence-based maximal quantum yield for PSII as a diagnostic of nutrient stress, J. Phycol., 37, 517-529, https://doi.org/10.1046/j.1529-8817.2001.037004517.x, 2001.

Pausch, F., Bischof, K., and Trimborn, S.: Iron and manganese co-limit growth of the Southern Ocean diatom *Chaetoceros debilis*, Plos One, 14, e0221959, https://doi.org/10.1371/journal.pone.0221959, 2019.

Price, N. M. and Morel, F. M. M.: Colimitation of phytoplankton growth by nickel and nitrogen, Limnol. Oceanogr., 36, 1071-1077, https://doi.org/10.4319/lo.1991.36.6.1071, 1991.

Price, N. M., Harrison, G. I., Hering, J. G., Hudson, R. J., Nirel, P. M., Palenik, B., and Morel, F. M.: Preparation and chemistry of the artificial algal culture medium Aquil, Biological Oceanography, 6, 443-461, https://doi.org/10.1080/01965581.1988.10749544, 1989.

Rogelj, J., Schaeffer, M., Friedlingstein, P., Gillett, N. P., van Vuuren, D. P., Riahi, K., Allen, M., and Knutti, R.: Differences between carbon budget estimates unravelled, Nat. Clim. Change, 6, 245-252, https://doi.org/10.1038/nclimate2868, 2016.

Saito, M. A., Moffett, J. W., and DiTullio, G. R.: Cobalt and nickel in the Peru upwelling region: a major flux of labile cobalt utilized as a micronutrient, Global Biogeochem. Cy., 18, 1-14, https://doi.org/10.1029/2003GB002216, 2004.

Schallenberg, C., Strzepek, R. F., Schuback, N., Clementson, L. A., Boyd, P. W., and Trull, T. W.: Diel quenching of Southern Ocean phytoplankton fluorescence is related to iron limitation, Biogeosciences, 17, 793-812, https://doi.org/10.5194/bg-17-793-2020, 2020.

Schuiling, R. D. and Krijgsman, P.: Enhanced weathering: an effective and cheap tool to sequester CO_2, Climatic Change, 74, 349-354, https://doi.org/10.1007/s10584-005-3485-y, 2006.

Sclater, F. R., Boyle, E., and Edmond, J. M.: On the marine geochemistry of nickel, Earth Planet Sc. Lett., 31, 119-

https://doi.org/10.5194/bg-2021-312
Preprint. Discussion started: 3 January 2022

128, https://doi.org/10.1016/0012-821X(76)90103-5, 1976.

Shilova, I. N., Mills, M. M., Robidart, J. C., Turk-Kubo, K. A., Björkman, K. M., Kolber, Z., Rapp, I., Van Dijken, G. L., Church, M. J., Arrigo, K. R., Achterberg, E. P., and Zehr, J. P.: Differential effects of nitrate, ammonium, and urea as N sources for microbial communities in the North Pacific Ocean, Limnol. Oceanogr., 62, 2550-2574, https://doi.org/10.1002/lno.10590, 2017.

Sieracki, M. E., Verity, P. G., and Stoecker, D. K.: Plankton community response to sequential silicate and nitrate depletion during the 1989 North Atlantic spring bloom, Deep-Sea Res. Pt. II, 40, 213-225, https://doi.org/10.1016/0967-0645(93)90014-E, 1993.

Suggett, D. J., Moore, C. M., Hickman, A. E., and Geider, R. J.: Interpretation of fast repetition rate (FRR) fluorescence: signatures of phytoplankton community structure versus physiological state, Mar. Ecol. Prog. Ser., 376, 1-19, https://doi.org/10.3354/meps07830, 2009.

Sunda, W. G.: Trace metal interactions with marine phytoplankton, Biological oceanography, 6, 411-442, 1989.

Taylor, L. L., Quirk, J., Thorley, R. M. S., Kharecha, P. A., Hansen, J., Ridgwell, A., Lomas, M. R., Banwart, S. A., and Beerling, D. J.: Enhanced weathering strategies for stabilizing climate and averting ocean acidification, Nature Clim. Change, 6, 402-406, https://doi.org/10.1038/nclimate2882, 2016.

Van Den Berg, C. M. G. and Nimmo, M.: Determination of interactions of nickel with dissolved organic material in seawater using cathodic stripping voltammetry, Sci Total Environ., 60, 185-195, https://doi.org/10.1016/0048-9697(87)90415-3, 1987.

Wafar, M., Le Corre, P., and l'Helguen, S.: f-Ratios calculated with and without urea uptake in nitrogen uptake by phytoplankton, Deep-Sea Res. Pt. I, 42, 1669-1674, https://doi.org/10.1016/0967-0637(95)00066-F, 1995.

Wolfe-Simon, F., Grzebyk, D., Schofield, O., and Falkowski, P. G.: The role and evolution of superoxide dismutases in algae, J. Phycol, 41, 453-465, https://doi.org/10.1111/j.1529-8817.2005.00086.x, 2005.

Xue, H. B., Jansen, S., Prasch, A., and Sigg, L.: Nickel speciation and complexation kinetics in freshwater by ligand exchange and DPCSV, Environ. Sci. Technol., 35, 539-546, https://doi.org/10.1021/es0014638, 2001.

Zamble, D., Rowińska-Żyrek, M., & Kozlowski, H. (Ed.): The Biological Chemistry of Nickel, The Royal Society of Chemistry, https://doi.org/10.1039/9781788010580, 2017.